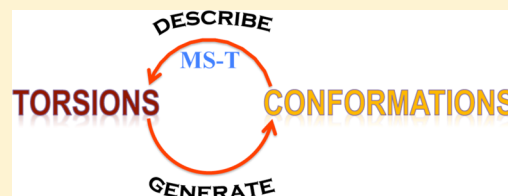


Quantum Thermochemistry: Multistructural Method with Torsional Anharmonicity Based on a Coupled Torsional Potential

Jingjing Zheng and Donald G. Truhlar*

Department of Chemistry, Chemical Theory Center, and Supercomputing Institute, University of Minnesota, Minneapolis, Minnesota 55455-0431, United States

ABSTRACT: We present a new approximation for calculating partition functions and thermodynamic functions by the multistructural method with torsional anharmonicity (MS-T). The new approximation is based on a reference potential with torsional barriers obtained from a calculation that includes local torsional coupling. By comparing to a fully coupled classical rotational-torsional partition function evaluated as a numerical phase space integral, the method is shown to provide improved accuracy in the classical limit. Quantum effects, which are most important at low temperatures, are included based on the harmonic approximation (which can be upgraded to a quasiharmonic approximation, that is, harmonic formulas with effective frequencies). Calculations were performed for six molecules (ethanol, 1-butanol, hexane, isohexane, heptane, and isoheptane), one radical (1-pentyl radical), and the saddle point structures of a hydrogen abstraction reaction (hydroxyl plus ethanol) to illustrate the difference between the new coupled-potential MS-T approximation and the original uncoupled-potential MS-T approximation. The new method improves the agreement with experimental results of calculated thermodynamic functions for 1-butanol, hexane, isohexane, and heptane.



1. INTRODUCTION

Torsional anharmonicity represents a difficult challenge when performing accurate thermochemical calculations for complex molecules.^{1–17} This is partly because multiple torsional degrees of freedom can lead to a large number of low-energy conformers that must be accounted for, but also because of the complexity of the coupling between torsions and other torsions, low-energy bending motions, and overall rotation. We have previously proposed a practical method¹⁸ for including torsional anharmonicity in thermochemical calculations on complex molecules; we called it the multistructural all-structures (MS-AS) method¹⁸ and later simplified the name to the multistructural method with torsional anharmonicity (MS-T).¹⁹ We use the latter name here. The objective of the MS-T method is to include the contribution of all conformational structures in a molecular partition function in a way that takes account of multiple-structure anharmonicity and torsional potential anharmonicity. To compute partition functions and thermodynamic functions, the MS-T method only requires geometries and Hessians of equilibrium conformational structures, and it implicitly estimates the conformational barrier heights by using the force constants of torsions in internal coordinates and an estimate of the local periodicities. In particular, the MS-T method does not require searching for saddle points that connect the conformational structures, mapping the connections between the saddle points and minima, or scanning the potential along any torsional coordinate. This makes the method efficient, and it allows one to use high-level electronic structure methods for the required energy and Hessian calculations. The MS-T method has been applied to quite a few molecules, e.g., pentyl radical,^{18,20} hexane and isohexane,²¹ heptane and isoheptane,²²

2-cyclohexylethyl radical,²³ 1-butanol,²⁴ 2-methyl-1-propanol,²⁴ butanal,²⁴ and 1-butoxyl radical.²⁵ The method has also been applied to transition states.^{20,23,25–30}

Note that the harmonic approximation includes kinetic and potential energy coupling—but only through quadratic terms. The original MS-T method recovers the local harmonic-oscillator approximation, or a quasiharmonic approximation, in the low-temperature limit and reaches the free-rotor limit of coupled torsional and rotational motions in the high-temperature limit; i.e., it includes kinetic and potential energy coupling at low T and kinetic energy coupling at high temperatures, where the torsional potential eventually becomes negligible. However, aside from the sum over structures and the switch between harmonic coupling and locally uncoupled torsions, the original MS-T method did not include potential energy coupling of the torsions in the intermediate-temperature regime. In this article, we propose an improved formulation of the MS-T method. This new formulation is motivated by the goal of using a coupled potential not only for normal-mode frequencies but also for an implicit estimation of effective torsional barriers. Therefore, the uncoupled internal-coordinate approximation used in the original MS-T method is eliminated in the new formulation. To distinguish the original and the new MS-T formulations, we label the original one as the MS-T approximation with effective barriers based on an uncoupled potential, or MS-T(U), and the new one as the MS-T approximation with effective barriers based on a coupled potential, or MS-T(C).

Received: December 7, 2012

Published: January 23, 2013

After presenting the new method, we apply it to several previously studied molecules for comparison with results obtained with the original method. We also apply it to transition state for an abstraction reaction. Note that the present method does not assume that torsions are separable or that they may be associated with individual normal modes. We apply the present methods to problems where such assignments are not valid and where even the number of structures differs from the number one would find in a separable model; separable models would be unreasonable for such problems.

2. THEORY

The acronyms are defined at first usage and summarized in the Nomenclature section at the end of the article.

2.1. Fully Coupled Classical Partition Function.

Consider a model system with t coupled (i.e., nonseparable) torsional modes. The exact classical partition function of such a system including overall rotations will be called the fully coupled classical-limit (FCC) result. It is given as

$$Q^{\text{FCC}} = \frac{8\pi^2}{\sigma_{\text{rot}}} \left(\frac{1}{2\pi\hbar^2\beta} \right)^{(t+3)/2} \int_0^{2\pi/\sigma_1} \dots \int_0^{2\pi/\sigma_t} e^{-\beta V(\phi_1, \dots, \phi_t)} [\det \mathbf{S}(\phi_1, \dots, \phi_t)]^{1/2} d\phi_1 \dots d\phi_t \quad (1)$$

where σ_{rot} is the symmetry number for overall rotation of the molecule, β is $1/k_B T$, k_B is Boltzmann's constant, T is temperature, \hbar is Planck's constant divided by 2π , ϕ_1, \dots, ϕ_t are torsion coordinates, $\sigma_1, \dots, \sigma_t$ are the torsional symmetry numbers, V is potential energy, and \mathbf{S} is the moment of inertia matrix for overall and internal rotation as worked out by Kilpatrick and Pitzer³¹ (KP). The \mathbf{S} matrix and its eigenspectrum depend on details of the coordinate system beyond just the torsional coordinates (a set of rotating frames must be defined as discussed elsewhere;^{19,31} however, the determinant of \mathbf{S} is uniquely defined by the torsional coordinates).

2.2. Moments of Inertia. In a fully coupled system, it is not possible to uniquely define moments of inertia associated with individual coordinates. Following Kilpatrick and Pitzer, we can use a congruent transformation (which preserves determinants but not the eigenspectrum) to block diagonalize the \mathbf{S} matrix to yield three one-dimensional blocks having elements equal to I_1^{rot} , I_2^{rot} , and I_3^{rot} , which are the principal moments of inertia associated with overall rotation of a rigid structure, and a t -dimensional block referred to as the Kilpatrick and Pitzer torsional moment of inertia matrix, \mathbf{D} . Thus,

$$|\mathbf{S}| = |\mathbf{D}| \prod_{i=1}^3 I_i^{\text{rot}} \quad (2)$$

and we will use the \mathbf{D} matrix in subsequent equations.

In addition to using $\det(\mathbf{D})$, that accounts fully for the kinetic energy coupling of torsions to each other and to overall rotational motion, we will also use a set of approximate torsional moments due to Pitzer³² that are obtained by treating each torsional degree of freedom independently. These approximate moments are denoted $I_{j,\tau}^{(U)}$, where (U) denotes that the moment of inertia is Pitzer's uncoupled one, τ denotes a particular uncoupled torsional coordinate about which rotation is being considered, and j denotes a particular structure j and its remaining torsional coordinates. Here, "structure" means a local minimum (i.e., a conformation) when we are

treating the partition function of a molecule and means a saddle point when we are treating a transition state hypersurface. The uncoupled Pitzer moments of inertia $I_{j,\tau}^{(U)}$ are equal to the diagonal elements of the \mathbf{D} matrix and are unique functions of the set of torsional angles. As will be seen in subsections 2.6 and 2.7, the Pitzer moments of inertia $I_{j,\tau}^{(U)}$ will only be used for methods based on uncoupled potentials, while only $\det(\mathbf{D})$ will be used for methods based on coupled potentials.

As a practical matter, we approximate the moments within a particular conformational basin as being constant; hence they are labeled by j and τ but are not functions of coordinates.

2.3. Torsional Frequencies. How to approximate torsional frequencies and barriers is a central question in developing methods for treating torsional anharmonicity. The barriers will be discussed in the next subsection; here we discuss the frequencies.

In order to affordably approximate the torsional potential in the vicinity of a structure j , we make use of approximate uncoupled local reference potentials. For this purpose, we define the local reference potential of torsion τ of structure j by

$$V_{j,\tau} = U_j + \frac{W_{j,\tau}}{2} [1 - \cos M_{j,\tau}(\phi_{j,\tau} - \phi_{j,\tau,\text{eq}})]; \quad \frac{-\pi}{M_{j,\tau}} \leq \phi_{j,\tau} - \phi_{j,\tau,\text{eq}} \leq \frac{\pi}{M_{j,\tau}} \quad (3)$$

where U_j is the potential energy of structure j relative to the global minimum or relative to the lowest-energy saddle point, $\phi_{j,\tau}$ is the torsional coordinate, $\phi_{j,\tau,\text{eq}}$ is the value of $\phi_{j,\tau}$ at the equilibrium or saddle point geometry of structure j , $W_{j,\tau}$ is the effective barrier on either side of $\phi_{j,\tau,\text{eq}}$, and $M_{j,\tau}$ is called the local periodicity of torsion τ . The physical meaning of the $M_{j,\tau}$ parameter has been extensively explained in the original MS-T paper.¹⁸ Our choice of the reference potential in eq 3 is a compromise between accuracy and affordability, and it allows calculations using only information about the geometries and Hessians of the local minimum structures without the need to characterize intervening barriers, to search for saddle points between the local minima, or even to carry out potential energy scanning along torsional coordinates. (When computing partition functions of transition states, one uses first order saddle points rather than local minima, but one does not need information about the second-order saddle points along the torsion coordinates of the transition states.)

In the original MS-T method,¹⁸ we evaluate the uncoupled torsional frequency $\omega_{j,\tau}^{(U)}$ (note that the symbol $\bar{\omega}_{j,\tau}$ is used in the original paper, but here we change the notation to make the relation to the new method more clear) for internal coordinate ϕ_τ as

$$\omega_{j,\tau}^{(U)} = \sqrt{F_{j,\tau\tau}/I_{j,\tau}} \quad (4)$$

where the force constant $F_{j,\tau\tau}$ is a diagonal element of the Wilson–Decius–Cross \mathbf{F}_j matrix and is nominally given by

$$F_{j,\tau\tau} = \frac{\partial^2 V_{j,\tau}}{\partial \phi_{j,\tau}^2} \quad (5)$$

which is independent of masses. However, in practice the internal-coordinate force constant matrix \mathbf{F}_j is calculated by³³

$$\mathbf{F}_j = \mathbf{A}_j^T \mathbf{F}_{\text{Cartesian},j} \mathbf{A}_j \quad (6)$$

where $\mathbf{F}_{\text{Cartesian},j}$ is the force constant in atomic Cartesian coordinates, and \mathbf{A}_j is the generalized inverse of the Wilson–Decius–Cross \mathbf{B}_j matrix. Note that \mathbf{B}_j and hence \mathbf{A}_j is rectangular because there are $3N$ atomic Cartesian coordinates but only $3N - 6$ linearly independent internal coordinates, where N is the number of atoms. If the generalized inverse of \mathbf{B}_j were calculated by singular value decomposition, it would be mass independent, but instead we calculate the generalized inverse of \mathbf{B}_j by³³

$$\mathbf{A}_j = \mathbf{u}\mathbf{B}_j^T(\mathbf{B}_j\mathbf{u}\mathbf{B}_j^T)^{-1} \quad (7)$$

where \mathbf{u} can be any matrix. In practice, we take \mathbf{u} to be a diagonal matrix with the reciprocals of the atomic masses as the diagonal elements, and as a consequence, \mathbf{F}_j does depend on the masses. The reason that we have chosen \mathbf{u} to be the reciprocal mass matrix is that this choice satisfies the Eckart–Sayvetz conditions^{34,35} for internal coordinates that carry no linear or angular momentum and therefore separate vibration from translation and rotation to the greatest extent possible. Since the vibrational and rotational kinetic energies depend on masses, this introduces a mass dependence, although in practice it is small.

Torsions in real molecules are often coupled, and the coupling affects the torsional frequencies and barriers. In a normal-mode analysis, it is often difficult to identify the torsional modes as they are coupled not only to each other but also to nontorsional modes. One way to consider torsion–torsion coupling is to drop the nontorsional rows and columns in the full Wilson–Decius–Cross³⁶ \mathbf{F}_j and \mathbf{G}_j^{-1} matrices. The full \mathbf{F}_j and \mathbf{G}_j^{-1} matrices can be written in terms of submatrices respectively as

$$\mathbf{F}_j = \begin{vmatrix} \mathbf{F}_j^{11} & \mathbf{F}_j^{12} \\ \mathbf{F}_j^{21} & \mathbf{F}_j^{22} \end{vmatrix} \quad \mathbf{G}_j^{-1} = \begin{vmatrix} \mathbf{Y}_j^{11} & \mathbf{Y}_j^{12} \\ \mathbf{Y}_j^{21} & \mathbf{Y}_j^{22} \end{vmatrix} \quad (8)$$

If the submatrices with label 22 are only associated with torsional coordinates, we define $\mathbf{F}_j^{\text{tor}} = \mathbf{F}_j^{22}$ and $\mathbf{G}_j^{\text{tor}} = (\mathbf{Y}_j^{22})^{-1}$. We label this kind of treatment of the mode coupling as primitive coupling (PC). Therefore, the primitively coupled torsional frequencies are given by $(\lambda_{j,\eta}^{(\text{PC})})^{1/2}$ where $\lambda_{j,\eta}^{(\text{PC})}$ is an eigenvalue of $\mathbf{G}_j^{\text{tor}}\mathbf{F}_j^{\text{tor}}$, and η denotes a coupled motion. We label the normal-mode analysis using $\mathbf{G}_j^{\text{tor}}\mathbf{F}_j^{\text{tor}}$ as a torsional normal-mode analysis.

Note that the determinant of the Kilpatrick and Pitzer \mathbf{D} matrix and the determinant of the $(\mathbf{G}_j^{\text{tor}})^{-1}$ matrix are the same. Using this fact simplifies the calculation by eliminating the need to define the rotation frames and connectivity of rotors in the input. Also, due to this relation, the determinant of the Kilpatrick and Pitzer moment of inertia matrix (which is all we need) is readily available in any program that has code to do vibrational analysis using the Wilson–Decius–Cross GF method.

However, it is not unusual for absolute values of matrix elements associated with the coupling of a torsional coordinate to a nontorsional coordinate in the full \mathbf{F} and \mathbf{G} matrices to be larger than absolute values of matrix elements within the torsional block. As a consequence, ignoring coupling between the torsional modes and the nontorsional modes can result in large changes in individual torsional frequencies. In contrast, the torsion–nontorsion couplings are usually much smaller than many of the diagonal elements associated with nontorsional coordinates; therefore ignoring the torsion–nontorsion

coupling elements will have much less of an effect on the nontorsional frequencies. Let us label the nontorsional frequencies as $\bar{\omega}_{j,\bar{m}}$ ($\bar{m} = 1, 2, \dots, F - t$); to calculate these frequencies, nonredundant internal coordinates for nontorsional modes are used to form the Wilson–Decius–Cross \mathbf{B}_j matrix for structure j , and this $(F-t) \times 3N$ dimensional \mathbf{B}_j matrix is used to construct the $\mathbf{G}_j^{\text{nontor}}$ and $\mathbf{F}_j^{\text{nontor}}$ matrices. The $\bar{\omega}_{j,\bar{m}}$ are the square roots of the eigenvalues of the $\mathbf{G}_j^{\text{nontor}}\mathbf{F}_j^{\text{nontor}}$ matrix.

We want our torsional frequencies to be consistent with the nontorsional frequencies discussed in the previous paragraph. Since the MS-T methods only need the product of the torsional frequencies, not their individual values, we achieve this consistency by approximating the product of coupled torsional frequencies as

$$\prod_{\eta=1}^t \omega_{j,\eta}^{(C)} = \frac{\prod_{m=1}^F \omega_{j,m}}{\prod_{\bar{m}=1}^{F-t} \bar{\omega}_{j,\bar{m}}} \quad (9)$$

where superscript (C) denotes the consistently coupled approximation. In the next subsection, we will use eq 9 for torsional frequencies instead of using primitively coupled frequencies.

2.4. Torsional Barriers. For the reference potential of eq 3, the second derivative of the potential at the stationary-point geometry (equilibrium structure or saddle point) gives

$$F_{j,\tau\tau} = \left. \frac{\partial^2 V_{j,\tau}}{\partial \phi_{j,\tau}^2} \right|_{\phi_{j,\tau} = \phi_{j,\tau,\text{eq}}} = \frac{W_{j,\tau}^{(U)}}{2} M_{j,\tau}^2 \quad (10)$$

where superscript (U) denotes the uncoupled barrier based on the uncoupled potential, which is

$$W_{j,\tau}^{(U)} = \frac{2F_{j,\tau\tau}}{M_{j,\tau}^2} \quad (11)$$

Note that torsional barrier is independent of the moments of inertia since it is a feature of the potential energy surface.

When torsions are coupled, we assume that each coupled torsion η has the reference potential form with the same form as eq 3 except that the coupled coordinate η is used, which is a linear combination of the uncoupled coordinate τ .

Similarly to eq 11, the barrier associated with the coupled reference potential might be taken as

$$W_{j,\eta}^{(C)} = \frac{2}{M_{j,\eta}^2} \frac{\partial^2 V_j}{\partial \phi_{j,\eta}^2} \quad (12)$$

However, it is difficult to obtain the local periodicity $M_{j,\eta}$ for the coupled motion η , and so we want to avoid assigning an $M_{j,\eta}$ to each eigenvector of the $\mathbf{F}_j^{\text{tor}}$ matrix in a practical calculation. Hence, we scale the $\mathbf{F}_j^{\text{tor}}$ matrix as

$$\tilde{\mathbf{F}}_j^{\text{tor}} = \mathbf{L}_j \mathbf{F}_j^{\text{tor}} \mathbf{L}_j \quad (13)$$

with the matrix \mathbf{L}_j being a diagonal matrix with elements given by $1/M_{j,\tau}$. Then, eq 12 for the coupled barrier is replaced by

$$W_{j,\eta}^{(C)} = 2\tilde{\lambda}_{j,\eta} \quad (14)$$

where $\tilde{\lambda}_{j,\eta}$ are the eigenvalues of the $\tilde{\mathbf{F}}_j^{\text{tor}}$ matrix. We emphasize that these effective barriers do not correspond to specific features of the true potential energy surface but instead enable us to model the accessible phase space in the vicinity of

structure j , which is important for obtaining accurate partition functions in the intermediate-temperature regime. This regime is not precisely defined, but we use this term to refer to temperatures where the average energies in the torsional modes are comparable to (neither much larger than nor much less than) the torsional barriers. Note that this occurs at different temperatures for different torsions, and the intermediate temperature regime for the molecule extends from where it is true for the lowest-energy barrier to where it is true for the highest-energy barrier.

The advantage of using effective barriers, eq 14, instead of actual torsional barriers is that the computation of the effective barrier heights requires minimal additional computational cost and human effort. In previous work,¹⁸ we showed for a simple case how one could use the actual torsional barriers in the multistructural method, but for complex molecules with strongly coupled torsions and a nonideal number of conformational structures, not only is it a considerable amount of work to search for, find, and optimize all the torsional saddle points, but it requires even more effort to assign the saddle points to specific structure-to-structure paths. The method presented in the present article does not require the assignment or even the search of any torsional barrier optimizations.

2.5. Reference Classical Partition Functions. We let J denote the number of conformational structures for a molecule or transition state. If we approximate the coupled potential in the vicinity of each structure by eq 3 with coupled torsional coordinate η , and if we approximate $\det(\mathbf{D}(\phi_1, \dots, \phi_t))$ in the vicinity of each structure by its value $\det(\mathbf{D}_j)$ at a local minimum or a saddle point of the potential energy, we may integrate eq 1 analytically to obtain^{9,37}

$$Q^{\text{MS-RC(C)}} = \sum_{j=1}^J q_j^{\text{RC(C)}} \quad (15)$$

where

$$q_j^{\text{RC(C)}} = \frac{8\pi^2}{\sigma_{\text{rot},j}} \left(\frac{1}{2\pi\hbar^2\beta} \right)^{3/2} (I_{j,1}^{\text{rot}} I_{j,2}^{\text{rot}} I_{j,3}^{\text{rot}})^{1/2} (\det \mathbf{D}_j)^{1/2} \times \prod_{\tau=1}^t \frac{\sqrt{2\pi/\beta}}{\hbar M_{j,\tau}} \prod_{\eta=1}^t \exp(-\beta W_{j,\eta}^{(\text{C})}/2) I_0(\beta W_{j,\eta}^{(\text{C})}/2) \quad (16)$$

where t is the number of torsions in the molecule or transition state and I_0 is a modified Bessel function. We call this the multistructural reference classical (RC) rotational-torsional partition function using coupled barrier heights and coupled moments of inertia, abbreviated MS-RC(C), where (C) denotes that coupled effective barriers and coupled moments of inertia are used.

If the $W_{j,\eta}^{(\text{C})}$ in eq 16 are replaced by the uncoupled effective barriers $W_{j,\eta}^{(\text{U})}$ calculated by eq 11, we obtain the multistructural reference classical rotational-torsional partition function using the uncoupled effective barrier heights, called MS-RC(UC), where (UC) denotes that uncoupled effective barriers and coupled moments of inertia are used. In particular, the MS-RC(UC) partition function is

$$Q^{\text{MS-RC(UC)}} = \sum_{j=1}^J q_j^{\text{RC(UC)}} \quad (17)$$

$$q_j^{\text{RC(UC)}} = \frac{8\pi^2}{\sigma_{\text{rot},j}} \left(\frac{1}{2\pi\hbar^2\beta} \right)^{3/2} (I_{j,1}^{\text{rot}} I_{j,2}^{\text{rot}} I_{j,3}^{\text{rot}})^{1/2} (\det \mathbf{D}_j)^{1/2} \times \prod_{\tau=1}^t \frac{\sqrt{2\pi/\beta}}{\hbar M_{j,\tau}} \prod_{\eta=1}^t \exp(-\beta W_{j,\eta}^{(\text{U})}/2) I_0(\beta W_{j,\eta}^{(\text{U})}/2) \quad (18)$$

If uncoupled Pitzer moments $I_{j,\tau}^{(\text{U})}$ and uncoupled effective barriers $W_{j,\tau}^{(\text{U})}$ are used, the MS-RC(UC) partition function reduces to the following formulas, denoted MS-RC(U):

$$Q^{\text{MS-RC(U)}} = \sum_{j=1}^J q_j^{\text{RC(U)}} \quad (19)$$

$$q_j^{\text{RC(U)}} = \frac{8\pi^2}{\sigma_{\text{rot},j}} \left(\frac{1}{2\pi\hbar^2\beta} \right)^{3/2} (I_{j,1}^{\text{rot}} I_{j,2}^{\text{rot}} I_{j,3}^{\text{rot}})^{1/2} \prod_{\tau=1}^t q_{j,\tau}^{\text{RC(U)}} \\ = \frac{8\pi^2}{\sigma_{\text{rot},j}} \left(\frac{1}{2\pi\hbar^2\beta} \right)^{3/2} (I_{j,1}^{\text{rot}} I_{j,2}^{\text{rot}} I_{j,3}^{\text{rot}})^{1/2} \times \prod_{\tau=1}^t \frac{\sqrt{2\pi I_{j,\tau}^{(\text{U})}/\beta}}{\hbar M_{j,\tau}} \exp(-\beta W_{j,\tau}^{(\text{U})}/2) I_0(\beta W_{j,\tau}^{(\text{U})}/2) \quad (20)$$

where the superscript (U) denotes that both the effective barriers and the moments of inertia are uncoupled. These three levels of approximation are of interest to show the differences between using various moments of inertia and effective barriers.

2.6. MS-T(U) Method. Here, we briefly review the MS-T(U) method.¹⁸ Note that the symbol (U) used for the MS-T method denotes the use of uncoupled torsional frequencies, uncoupled effective torsional barriers, and uncoupled moments of inertia, but the coupling between frequencies and coupling between moments of inertia are considered in a factor Z_j that will be discussed below. The conformational-rovibrational partition function of the MS-T(U) method is

$$Q_{\text{con-rovib}}^{\text{MS-T(U)}} = \sum_{j=1}^J Q_{\text{rot},j} \exp(-\beta U_j) Q_j^{\text{HO}} Z_j \prod_{\tau=1}^t f_{j,\tau} \quad (21)$$

$$Q_{\text{rot},j} = \frac{\sqrt{\pi}}{\sigma_{\text{rot},j}} \left(\frac{2}{\hbar^2\beta} \right)^{3/2} \sqrt{I_{j,1}^{\text{rot}} I_{j,2}^{\text{rot}} I_{j,3}^{\text{rot}}} \quad (22)$$

where $Q_{\text{rot},j}$ is the classical rotational partition function of structure j , $\sigma_{\text{rot},j}$ is overall rotational symmetry number associated with a specific structure j , Q_j^{HO} is the usual normal-mode harmonic oscillator vibrational partition function calculated at structure j , Z_j is a factor designed to ensure that the MS-T(U) partition function reaches the correct high-temperature limit, and $f_{j,\tau}$ is an internal-coordinate torsional anharmonicity function that, in conjunction with Z_j , adjusts the harmonic results of structure j for the presence of the torsional motion associated with coordinate τ .

If desired, Q_j^{HO} , while still based on the HO formula, may be employed with scaled high frequencies³⁸ and/or increased low frequencies^{39–41} as an approximate way to include some of the effects of anharmonicity; then it can be called quasiharmonic instead of harmonic.

The reference Pitzer–Gwinn (RPG) method^{9,37} is used to calculate the factor $f_{j,\tau}$ for torsion τ by using the reference potential defined in eq 3. The factor $f_{j,\tau}$ is written as

$$f_{j,\tau} = \frac{q_{j,\tau}^{\text{RC(U)}}}{q_{j,\tau}^{\text{CHO(U)}}} \quad (23)$$

$$q_{j,\tau}^{\text{CHO(U)}} = \frac{1}{\hbar\beta\omega_{j,\tau}^{(\text{U})}} \quad (24)$$

where $q_{j,\tau}^{\text{CHO(U)}}$ and $q_{j,\tau}^{\text{RC(U)}}$ are the classical harmonic-oscillator partition function and reference classical partition function of torsion τ for structure j using uncoupled torsional frequencies and uncoupled torsional effective barriers, respectively.

Equations 4, 11, 20, 23, and 24 then yield

$$f_{j,\tau} = \frac{\omega_{j,\tau}^{(\text{U})} \sqrt{2\pi\beta I_{j,\tau}}}{M_{j,\tau}} \exp(-\beta I_{j,\tau} (\omega_{j,\tau}^{(\text{U})})^2 / M_{j,\tau}^2) \times I_0(\beta I_{j,\tau} (\omega_{j,\tau}^{(\text{U})})^2 / M_{j,\tau}^2) \quad (25)$$

or equivalently

$$f_{j,\tau} = \sqrt{\pi\beta W_{j,\tau}^{(\text{U})}} \exp(-\beta W_{j,\tau}^{(\text{U})}/2) I_0(\beta W_{j,\tau}^{(\text{U})}/2) \quad (26)$$

We label the MS method as the MS-LH (local harmonic) method when all $f_{j,\tau}$ and Z_j are set to 1. (This would be MS-LQ if one uses quasiharmonic frequencies, as mentioned above.) The MS-LH (or MS-LQ) method is mainly used for comparison purposes to see the effects of the $f_{j,\tau}$ and Z_j factors.

It is useful to rewrite the product of the $f_{j,\tau}$ factors as

$$\prod_{\tau=1}^t f_{j,\tau} = \prod_{\tau=1}^t \hbar\beta\omega_{j,\tau}^{(\text{U})} \prod_{\tau'=1}^t \frac{\sqrt{2\pi I_{j,\tau'}^{(\text{U})}}}{\hbar M_{j,\tau'}} \exp(-\beta W_{j,\tau'}^{(\text{U})}/2) \times I_0(\beta W_{j,\tau'}^{(\text{U})}/2) \quad (27)$$

Equation 27 indicates that the product of the $f_{j,\tau}$ factors can be refactored into a product of reciprocal classical harmonic oscillator partition functions labeled with τ and a product of classical reference potential partition functions labeled with τ' . Therefore, one does not need to associate specific τ factors with specific τ' factors; we will use this feature in section 2.7.

To ensure that calculations reach the correct high-temperature limit, which is determined by the kinetic coupling in the KP moment of inertia matrix, two adjustments were made in the MS-T(U) method. One is to replace the normal-mode partition function in the high- T limit by an internal-coordinate one, and the other is to correct for kinetic energy coupling of torsions to one another. In the MS-T(U) method, we use a factor Z_j to account for these two corrections averaged over all the torsions in a structure. In particular, we use

$$Z_j = g_j + (1 - g_j) Z_j^{\text{int}, \text{coup}} \quad (28)$$

where

$$Z_j^{\text{int}} = \frac{\prod_{\bar{m}=1}^{F-t} \bar{\omega}_{j,\bar{m}}^{-1} \prod_{\tau=1}^t (\omega_{j,\tau}^{(\text{U})})^{-1}}{\prod_{m=1}^F \omega_{j,m}^{-1}} \quad (29)$$

$$Z_j^{\text{coup}} = \left(\frac{\det \mathbf{D}_j}{\prod_{\tau=1}^t I_{j,\tau}^{(\text{U})}} \right)^{1/2} \quad (30)$$

and

$$g_j = \left(\prod_{\tau=1}^t \tanh \left(\frac{\omega_{j,\tau}^{(\text{U})} \sqrt{2\pi\beta I_{j,\tau}}}{M_{j,\tau}} \right) \right)^{1/t} \quad (31)$$

If the modes were uncoupled, it would be preferable to make corrections for each torsion individually, i.e., to change Z_j to a product of $Z_{j,\tau}$ in eq 21, because each torsion would reach the high- T limit at a different rate, depending primarily on the heights of the conformational barriers. However, this is not possible because the modes are coupled in most cases. This problematic issue is one motivation for the present work, and the MS-T(C) method presented in the next subsection represents an attempt to improve on this situation.

2.7. MS-T(C) Method. In this subsection, we present an approach designed to account for torsional potential coupling in the effective barriers that determine the behavior at intermediate temperatures while availing ourselves of a functional form for the reference classical potential that has qualitatively correct behavior in the high- T limit, without requiring individual effective barriers to correspond to features on the true potential energy surface. For this purpose, we rewrite the MS-T(U) formula to eliminate the need for using the switching functions Z_j to reach the correct limits. We also eliminate the approximation using locally uncoupled internal-coordinate potentials for calculating torsional frequencies and effective barriers so that the final result will not involve $\omega_{j,\tau}^{(\text{U})}$ and $I_{j,\tau}^{(\text{U})}$.

The new formula has three major changes: (1) A set of coupled effective torsional barriers $W_{j,\eta}^{(\text{C})}$ replaces the uncoupled effective torsional barriers $W_{j,\tau}^{(\text{U})}$. (2) The classical harmonic oscillator limit for the torsional degrees of freedom is approximated using the consistently coupled torsional frequencies. (3) The product of uncoupled Pitzer moments of inertia $I_{j,\tau}^{(\text{U})}$ are replaced by the $\det(\mathbf{D})$, instead of relying on the Z_j^{coup} term of eq 30 to be switched on as the temperature is increased by the switching function of eq 31. Therefore, the (C) superscript used to denote the MS-T method denotes using the consistently coupled frequencies, the coupled effective torsional barriers, and the coupled moments of inertia.

The MS-T(C) conformational-rovibrational partition function is written as

$$Q_{\text{con-rovib}}^{\text{MS-T(C)}} = \sum_{j=1}^J Q_{\text{rot},j} \exp(-\beta U_j) Q_j^{\text{HO}} \prod_{\eta=1}^t f_{j,\eta} \quad (32)$$

In contrast to the MS-T(U) scheme, the torsional anharmonicity factors $f_{j,\eta}$ will represent corrections to a set of coupled motions, i.e., combinations of torsional coordinates as discussed further below, and indexed by η instead of a single torsional coordinate τ . Because the torsional coordinates are now treated as coupled, the product of all t anharmonicity factors is treated together. In particular, we define

$$\prod_{\eta=1}^t f_{j,\eta} = \prod_{\eta=1}^t \frac{q_{j,\eta}^{\text{RC(C)}}}{q_{j,\eta}^{\text{CHO(C)}}} \quad (33)$$

where $q_{j,\eta}^{\text{CHO(C)}}$ and $q_{j,\eta}^{\text{RC(C)}}$ are the classical harmonic oscillator partition function and reference classical partition function of the coupled torsional motion η for structure j using consistently coupled torsional frequencies and coupled effective torsional barriers, respectively. The product of the $q_{j,\eta}^{\text{RC(C)}}$ factors is

$$\prod_{\eta=1}^t q_{j,\eta}^{\text{RC(C)}} = \sqrt{\det(\mathbf{D}_j)} \prod_{\tau=1}^t \frac{\sqrt{2\pi/\beta}}{\hbar M_{j,\tau}} \prod_{\eta=1}^t \exp(-\beta W_{j,\eta}^{(\text{C})}/2) I_0(\beta W_{j,\eta}^{(\text{C})}/2) \quad (34)$$

We then use eq 9 to approximate the product of the coupled classical harmonic limits of the reference classical expression as

$$\prod_{\eta=1}^t \frac{1}{q_{j,\eta}^{\text{CHO(C)}}} = (\hbar\beta)^t \frac{\prod_{m=1}^F \omega_{j,m}}{\prod_{\bar{m}=1}^{F-t} \bar{\omega}_{j,\bar{m}}} \quad (35)$$

We note that the coupled torsional coordinates associated with the calculation of the $W_{j,\eta}^{(\text{C})}$ are not identical to the normal mode coordinates associated with the solution of the torsional normal-mode analysis, so eq 33 only approximately reproduces the classical harmonic limit of the coupled effective reference potentials, but it is expected to be close provided the coupled effective potentials are reasonable. Using eqs 34 and 35, the product of the $f_{j,\eta}$ can be written as

$$\prod_{\eta=1}^t f_{j,\eta} = (2\pi\hbar\beta)^{t/2} \frac{\prod_{m=1}^F \omega_{j,m}}{\prod_{\bar{m}=1}^{F-t} \bar{\omega}_{j,\bar{m}}} \frac{\sqrt{\det \mathbf{D}_j}}{\prod_{\tau=1}^t M_{j,\tau}} \prod_{\eta=1}^t \exp(-\beta W_{j,\eta}^{(\text{C})}/2) I_0(\beta W_{j,\eta}^{(\text{C})}/2) \quad (36)$$

In contrast to the torsional anharmonicity factors in the MS-T(U) method, eq 36 does not approach 1 in the low- T limit, so the MS-T(U) scheme does not approach the harmonic oscillator limit at low- T but instead approaches a limit that is more consistent with separating the torsions from the nontorsional modes in order to include the torsional anharmonicity more fully.

Equation 33 shows that the ratio in $f_{j,\eta}$ is a factor that corrects the HO approximation for anharmonicity. At first examination, it could appear inconsistent in that $q_{j,\eta}^{\text{CHO(C)}}$ in the denominator is based on normal mode coordinates whose determination involves simultaneous consideration of kinetic and potential coupling, whereas $q_{j,\eta}^{\text{RC(C)}}$ in the denominator involves treating kinetic coupling and potential coupling separately by \mathbf{D}_j and $W_{j,\eta}^{(\text{C})}$, respectively. However, one can look at it in a different way. For this purpose, it is informative to conceptually rewrite the MS-T(C) formula as

$$Q_{\text{con-rovib}}^{\text{MS-T(C)}} = \sum_{j=1}^J Q_{\text{rot},j} \exp(-\beta U_j) Q_j^{\text{HO,nontor}} \prod_{\eta=1}^t q_{j,\eta}^{\text{RC(C)}} \left(\frac{Q_j^{\text{HO,tor}}}{\prod_{\eta=1}^t q_{j,\eta}^{\text{CHO(C)}}} \right) \quad (37)$$

where we suppose the quantum HO partition function can be partitioned into a torsional part $Q_j^{\text{HO,tor}}$ and a nontorsional part $Q_j^{\text{HO,nontor}}$, i.e., $Q_j^{\text{HO}} = Q_j^{\text{HO,nontor}} Q_j^{\text{HO,tor}}$. Since the normal modes do not separate into strictly torsional modes and strictly nontorsional modes, this is just schematic, but it shows how the kinetic and potential coupling in the denominator and numerator are consistent, i.e., they both consider kinetic coupling and potential coupling simultaneously. In particular the MS-T(C) method can be viewed as the torsional modes being treated by the quantal HO approximation and the nontorsional modes being treated by the classical RC

approximation corrected for quantal effects by a Pitzer–Gwinn type correction (the final ratio in eq 37).

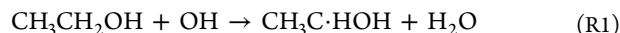
To calculate the thermodynamic functions from the partition function, we need the partial derivative of the logarithm of the partition function with respect to β :

$$-\frac{\partial}{\partial \beta} \ln Q_{\text{con-rovib}}^{\text{MS-T(C)}} = \frac{1}{Q_{\text{con-rovib}}^{\text{MS-T(C)}}} \sum_{j=1}^J (Q_{\text{rot},j} \exp(-\beta U_j) Q_j^{\text{HO}} \prod_{\eta=1}^t f_{j,\eta}) \left\{ \frac{3}{2\beta} + U_j + \sum_{m=1}^F \frac{\hbar\omega_{j,m}}{2} \left(\frac{1 + e^{-\beta\hbar\omega_{j,m}}}{1 - e^{-\beta\hbar\omega_{j,m}}} \right) + \sum_{\eta=1}^t \left[\frac{W_{j,\eta}^{(\text{C})}}{2} \left(1 - \frac{I_1(\beta W_{j,\eta}^{(\text{C})}/2)}{I_0(\beta W_{j,\eta}^{(\text{C})}/2)} \right) - \frac{1}{2\beta} \right] \right\} \quad (38)$$

3. COMPUTATION

We applied the MS-T(U) and MS-T(C) formulas to some previously studied cases. For comparison purposes, we calculated partition functions and thermodynamic functions of ethanol,²⁸ 1-butanol,²⁴ 1-pentyl radical,¹⁸ hexane,²¹ isohexane,²¹ heptane,²² and isoheptane²² using the same potential energy surfaces as used in our previous studies. The methods used for calculating the potential energy surfaces and the number of structures observed in each case are listed in Table 1.

In order to evaluate the accuracy of the MS-T(C) formula, we calculated rotational-torsional partition functions of pentane and the multistructural conventional transition state of the reaction R1²⁸ (denoted R1 TS)



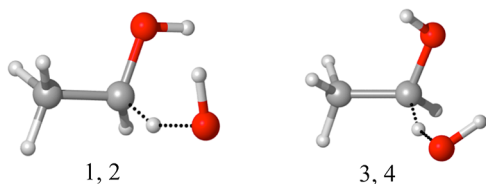
using the FCC method and compared them to MS-RC(U), MS-RC(UC), and MS-RC(C) results. The structures of R1 TS are shown in Figure 1. The high-frequency vibrational motions omitted in this comparison are well approximated by the harmonic oscillator expression, and quantum effects for the low-frequency torsional motions are fairly small for temperature 200 K and above and likely to be well estimated by the Pitzer–Gwinn type approximation inherent in the full-dimensional MS-T approximations, so these reduced-dimensional comparisons are expected to be representative of the accuracy of the two full-dimensional MS-T approximations. The kinetics of reaction R1 is beyond the scope of this paper, and only partition functions for the R1 transition state are calculated.

Because of the high computational cost of the FCC method, we used the MPW1K/6-31G(d) method to calculate the potential energy surfaces for pentane and the R1 TS. In the FCC, MS-RC(C), MS-RC(UC), and MS-RC(U) calculations on these systems, only torsional coordinates are relaxed, and the other degrees of freedom are held fixed at the values in the global minimum structure in order to further reduce the computational cost. The pentane and R1 TS cases each have four torsions. The integrals are calculated using a grid with torsional nodes separated by 18°. We integrate each dimension from 0 to 2π using the repeated trapezoidal rule, and then the integral is divided by the product of the torsional symmetry numbers. A total of 160 000 single-point energies were

Table 1. Methods Used for Calculating Potential Energy Surfaces for the Cases Studied

system	no. of structures		method ^b	reference
	actual	ideal ^a		
ethanol	3	3	CCSD(T)-F12b/may-cc-pVQZ//M08-HX/MG3S	28
1-pentyl	15	27	M06-2X/MG3S	18
1-butanol	29	27	CCSD(T)-F12a/jul-cc-pVTZ//M08-HX/MG3S	24
hexane	23	27	CCSD(T)-F12a/jul-cc-pVTZ//M06-2X/MG3S	21
isohexane	13	9	CCSD(T)-F12a/jul-cc-pVTZ//M06-2X/MG3S	21
heptane	58	81	CCSD(T)-F12a/jul-cc-pVTZ//M06-2X/MG3S	22
isoheptane	37	27	CCSD(T)-F12a/jul-cc-pVTZ//M06-2X/MG3S	22
pentane	7	9	MPW1K/6-31G(d) ^a	this work
R1 TS	4	18	MPW1K/6-31G(d) ^a	this work

^aFor alkanes and alcohols, the ideal number of conformational structures is calculated by assuming that, when R is not H, an $\text{RH}_2\text{CCR}_2\text{H}_2$ torsion or an $\text{RH}_2\text{CCR}_2\text{H}$ torsion generates three structures, and an $\text{HO}-\text{CH}_2\text{R}$ torsion also generates three structures. (When R is H, no new structures are generated.) In 1-pentyl, the local periodicity (M value) for $\bullet\text{CH}_2-\text{CH}_2\text{R}$ is 6 for some structures, and this torsion has symmetry 2, so the ideal number of distinguishable structures is taken as 3. For the transition state, the C–O torsion OH in the ethanol moiety generates three structures, and because the angle between two partial bonds is close to 180° , one may assume that the other two torsions would ideally generate the same three structures. This brings the number of structures up to nine. But the other H in the CH_2 group can also be abstracted, and this brings in another nine structures, so the ideal total number of structures is taken as 18. ^bThe references for the electronic structure methods and basis sets are as follows (given in parentheses): CCSD(T)-F12a and CCSD(T)-F12b (44–46), M08-HX (47), M06-2X (48), MPW1K (49), MG3S (50), may-cc-pVQZ and jul-cc-pVTZ (51,52), and 6-31G(d) (53).

**Figure 1.** Saddle points of R1. Only one structure of a pair of mirror images is shown.

calculated by the MPW1K/6-31G(d) method for each FCC calculation.

All the partition function and thermodynamic function calculations were carried out by a modified version of the *MSTor*^{19,42} program. The MPW1K/6-31G(d) calculations were performed using the *Gaussian09*⁴³ program.

4. RESULTS AND DISCUSSION

Table 1 shows the actual number of structures for each system as obtained by exhaustive conformational searching, and it also shows the ideal number of structures obtained by assuming that torsions are uncoupled. Except for ethanol (with only two torsions), the uncoupled torsion model cannot predict the correct number of conformational structures. Furthermore, in all cases (even ethanol), it is not possible to assign all the

torsions to individual normal modes. Therefore a method based on an uncoupled (separable) torsional model is not applicable to any of the present systems.

One of the major difficulties in developing a practical method to treat torsions for complex systems is that it is, in most cases, impossible to identify torsional motions with specific normal modes. In redesigning the MS-T method to better incorporate torsional coupling we exploit the facts that we only need the product of the torsional frequencies rather than individual frequencies and the determinant of KP moments of inertia matrix rather than moments of inertia for each torsion. As explained above, the MS-T(C) method approximates the product of the torsional frequencies as the ratio of the product of normal-mode frequencies to the product of the torsion-projected normal-mode frequencies. In the limit of no interaction between torsional modes and nontorsional modes, this approximation will give the exact values of the product of the torsional frequencies. Table 2 lists the six lowest nontorsional vibrational frequencies obtained by normal-mode analysis (ω) and by torsion-projected normal-mode analysis ($\bar{\omega}$) for the global minimum of various species. In Table 2, six normal-mode frequencies ω were selected to best match the six lowest $\bar{\omega}$. The ratio of the product of the six ω to the product of the six $\bar{\omega}$ will be 1 if there is no interaction between torsional and nontorsional modes. Table 2 shows that these ratios are very close to 1 with a maximum observed deviation of 12%, indicating that neglecting the coupling between the torsional and nontorsional modes has only a small impact on the nontorsional frequencies calculated by eq 9.

The classical partition functions for overall and internal rotation are calculated for pentane and the saddle points of R1 by the fully coupled classical integral as benchmarks for evaluating the accuracy of the MS-RC methods. Since the MS-RC formalism is also used in the MS-T methods, this evaluation can also be viewed as a test of a key element of the MS-T methods.

Pentane has a rotational symmetry number of 2, which is used in eq 1. In the MS-RC(C), MS-RC(UC), and MS-RC(U) calculations, seven distinguishable structures are included, and the rotational symmetry numbers $\sigma_{\text{rot},j}$ used in MS-RC are determined by the symmetry group of structure j .

The saddle points of reaction R1 consist of two pairs of mirror images. Because the saddle points of R1 have a chiral center, the members of a pair of mirror images cannot be interconverted by internal rotations. Therefore, the direct classical integral can only cover the contribution from two saddle points; the integral results are doubled to account for the contributions from the mirror image saddle points when tabulating partition functions.

The effective torsional barriers calculated by using both the coupled and uncoupled potentials for pentane and the R1 TS are listed in Table 3. The coupled and uncoupled barriers are quite different for the R1 TS case. To further understand the effective barrier calculations, we consider the simplest case in this study, ethanol. There is more than one way to calculate torsional barriers. One way is to calculate barriers using eq 12 and using a geometrical mean of $M_{j,\tau}$ values for all torsions. The second derivative of potential with respect to coupled torsional coordinate $\phi_{j,\tau}$ ($\partial^2 V_j / (\partial \phi_{j,\tau}^2)$), can be calculated using the chain rule. Note that the coupled torsional coordinate $\phi_{j,\tau}$ is a linear combination of the uncoupled coordinates $\phi_{j,\tau'}$ and this linear combination is provided by the eigenvector of the $\mathbf{G}_j^{\text{tor}} \mathbf{F}_j^{\text{tor}}$ matrix. In this way, we obtained the two torsional barriers in

Table 2. The Six Lowest Nontorsional Vibrational Frequencies Calculated by Normal Mode Analysis (ω) and by Torsion-Projected Normal Mode Analysis ($\bar{\omega}$) for the Global Minimum of Various Species

method	frequency (cm ⁻¹)						ratio ^a
ethanol							
ω	405.8	790.4	889.1	1018.4	1100.2	1146.6	1.00
$\bar{\omega}$	405.8	788.4	889.1	1018.4	1100.2	1146.5	
1-butanol							
ω	261.4	335.8	494.8	718.0	817.4	835.4	1.08
$\bar{\omega}$	242.5	334.7	494.4	716.2	817.4	835.3	
1-pentyl							
ω	250.3	328.0	434.9	480.1	721.4	786.8	1.04
$\bar{\omega}$	243.8	326.9	433.5	479.8	719.7	786.7	
hexane							
ω	127.7	290.1	361.1	455.8	706.9	721.3	1.00
$\bar{\omega}$	127.7	290.1	361.1	455.8	705.3	719.7	
isohexane							
ω	177.5	319.9	370.0	431.1	441.5	723.7	1.01
$\bar{\omega}$	182.0	312.6	368.3	430.5	440.5	722.1	
heptane							
ω	97.9	242.1	300.4	413.2	477.5	712.9	1.00
$\bar{\omega}$	97.9	242.1	300.4	413.2	477.5	713.9	
isoheptane							
ω	147.5	297.0	306.0	405.6	433.8	473.0	1.12
$\bar{\omega}$	136.8	294.1	298.9	403.8	432.6	472.9	

^aThe ratio is $\prod_{m=1}^6 \omega_m / \prod_{\bar{m}=1}^6 \bar{\omega}_{\bar{m}}$.

Table 3. Effective Torsional Barriers (in kcal/mol) Calculated by Coupled and Uncoupled Potentials for Pentane and for the R1 Saddle Point, the Determinant of the D Matrix (in amu⁴ Å⁸), and the Product of Pitzer Moments of Inertia, $\Pi_{\tau} I_{j,\tau}$ (in amu⁴ Å⁸)

species	torsional barriers								D	$\Pi I_{\tau,j,\tau}^{(U)}$
	uncoupled				coupled					
pentane ^a										
TT	3.0	3.0	3.2	3.2	2.5	2.9	3.3	3.7	1034.5	1228.4
GG/G ⁻ G ⁻	3.5	3.5	5.5	5.5	3.0	3.4	4.3	7.3	1810.9	3306.7
TG/TG ⁻	2.8	3.0	3.3	3.5	1.7	2.8	3.2	4.9	1465.3	1696.7
G ⁻ T/GT	2.8	3.0	3.3	3.5	1.7	2.8	3.2	4.9	1465.3	1696.7
X ⁻ G/XG ⁻	3.3	3.4	4.1	4.5	2.1	3.3	3.8	6.0	2080.1	2418.9
G ⁻ X/GX ⁻	3.3	3.4	4.1	4.5	2.1	3.3	3.8	6.0	2080.1	2418.9
R1 SP										
1, 2	2.8	3.3	3.6	12.7	0.2	2.8	4.6	14.8	0.3912	2.435
3, 4	3.3	3.6	3.8	8.4	0.2	3.3	3.6	12.0	0.2916	2.162

^aPentane conformational structures are denoted by the two CCCC torsion angles. The “T” is for trans, G or G⁻ is for gauche torsion angles around 60° or -60°, and X or X⁻ is for “cross” or “perpendicular” angles of about 90° or -90°.

ethanol (methyl group rotation and hydroxyl group rotation) as 2.3 and 1.3 kcal/mol respectively. However, explicit saddle point optimizations by the M08-HX/MG3S method give the two barriers as 3.0 and 1.1 kcal/mol. The 2.3 kcal/mol barrier from the coupled coordinates is quite different with the 3.0 kcal/mol barrier by optimization. It is because one eigenvector of the $\mathbf{G}_j^{\text{tor}} \mathbf{F}_j^{\text{tor}}$ matrix has two modes almost equivalently mixed, and therefore the corresponding barrier gets averaged over two uncoupled barriers. The barriers calculated by both the uncoupled method (eq 11) and the coupled method (eq 14) are 3.1 and 1.0 kcal/mol. These results indicate that the two torsions are almost separable on the potential energy surface, but they are strongly mixed in normal mode coordinates by the atomic-mass-dependent kinetic coupling; such strong mixing in describing torsional motions is unphysical because the potential energy surface is strictly independent of the atomic masses. This example also further rationalizes the scheme that separates

the kinetic coupling and potential coupling in calculating the $q_{j,\eta}^{\text{RC}(C)}$.

The determinants of the **D** matrices and the products of the Pitzer moments of inertia are also listed in Table 3. These two quantities are close to each other for pentane, but they differ by a factor of 6.2 or 7.4 for the R1 TS. These large differences show the strong kinetics coupling between the torsional modes. The effect of these differences on the partition function would be smaller though because the partition function depends on the square root of det(**D**).

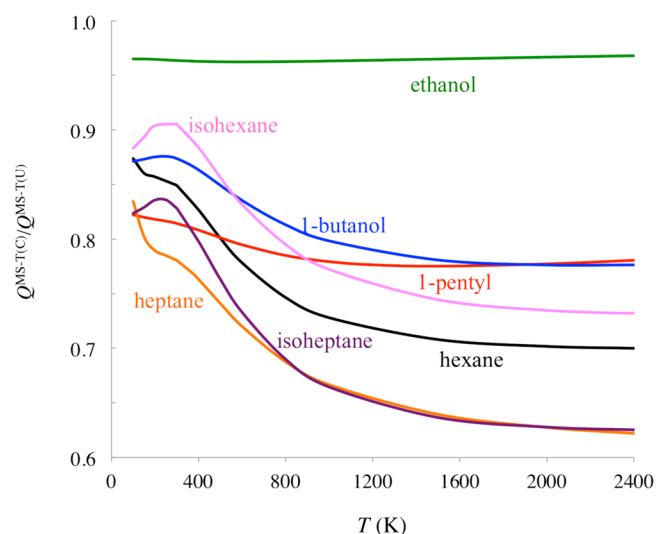
The classical partition functions calculated by the FCC, MS-RC(U), MS-RC(UC), and MS-RC(C) methods are listed in Table 4. For pentane, the MS-RC(C) partition functions based on the coupled barriers and coupled moments of inertia agree well with those obtained by the FCC integral prescription. For the R1 TS, the MS-RC(C) partition functions significantly improve the MS-RC(UC) results compared with the FCC ones. For example, the MS-RC(C) method improves the MS-

Table 4. Rotational-Torsional Partition Function Calculated by the Fully Coupled Classical Integral and by the MS-RC Methods for Pentane and the R1 Saddle Points

T (K)	FCC	MS-RC(C)	MS-RC(UC)	MS-RC(U)
pentane				
200	2.45×10^4	2.53×10^4	2.34×10^4	2.55×10^4
250	1.06×10^5	1.10×10^5	1.00×10^5	1.09×10^5
298	3.40×10^5	3.56×10^5	3.20×10^5	3.49×10^5
400	2.41×10^6	2.55×10^6	2.27×10^6	2.49×10^6
500	1.05×10^7	1.11×10^7	1.00×10^7	1.10×10^7
600	3.41×10^7	3.65×10^7	3.31×10^7	3.66×10^7
700	9.07×10^7	9.75×10^7	8.97×10^7	9.93×10^7
800	2.08×10^8	2.25×10^8	2.09×10^8	2.32×10^8
900	4.26×10^8	4.63×10^8	4.35×10^8	4.83×10^8
1000	7.99×10^8	8.73×10^8	8.27×10^8	9.20×10^8
1500	7.93×10^9	8.91×10^9	8.64×10^9	9.67×10^9
1800	2.09×10^{10}	2.38×10^{10}	2.32×10^{10}	2.61×10^{10}
2000	3.60×10^{10}	4.12×10^{10}	4.04×10^{10}	4.54×10^{10}
2400	8.95×10^{10}	1.03×10^{11}	1.02×10^{11}	1.15×10^{11}
5000	2.59×10^{12}	3.04×10^{12}	3.03×10^{12}	3.44×10^{12}
10000	4.50×10^{13}	5.22×10^{13}	5.22×10^{13}	5.94×10^{13}
50000	1.89×10^{16}	2.08×10^{16}	2.08×10^{16}	2.37×10^{16}
90000	1.56×10^{17}	1.69×10^{17}	1.69×10^{17}	1.93×10^{17}
R1 transition state				
200	2.38×10^4	1.79×10^4	5.41×10^3	1.35×10^4
250	8.87×10^4	5.93×10^4	1.95×10^4	4.89×10^4
298	2.53×10^5	1.54×10^5	5.46×10^4	1.37×10^5
400	1.48×10^6	7.72×10^5	3.17×10^5	7.98×10^5
500	5.61×10^6	2.66×10^6	1.23×10^6	3.10×10^6
600	1.64×10^7	7.35×10^6	3.72×10^6	9.44×10^6
700	3.99×10^7	1.73×10^7	9.48×10^6	2.41×10^7
800	8.49×10^7	3.61×10^7	2.12×10^7	5.40×10^7
900	1.63×10^8	6.88×10^7	4.27×10^7	1.09×10^8
1000	2.89×10^8	1.22×10^8	7.94×10^7	2.03×10^8
1500	2.35×10^9	1.04×10^9	8.00×10^8	2.06×10^9
1800	5.72×10^9	2.65×10^9	2.16×10^9	5.57×10^9
2000	9.42×10^9	4.49×10^9	3.77×10^9	9.76×10^9
2400	2.18×10^{10}	1.10×10^{10}	9.69×10^9	2.51×10^{10}
5000	5.01×10^{11}	3.27×10^{11}	3.16×10^{11}	8.20×10^{11}
10000	7.51×10^{12}	5.89×10^{12}	5.84×10^{12}	1.52×10^{13}
50000	2.66×10^{15}	2.50×10^{15}	2.50×10^{15}	6.51×10^{15}
90000	2.13×10^{16}	2.06×10^{16}	2.06×10^{16}	5.35×10^{16}

RC(UC) by a factor 3.3, 2.4, and 1.5 at 200, 400, and 1000 K, respectively. However, the MS-RC(C) partition functions are still underestimates of the accurate results. Note that the estimated barriers are based on a simple cosine potential, and the moments of inertia at minima are used to represent those continuously changed moments of inertia in the accessible phase space. The large difference between the $\det(\mathbf{D})$ and the product of the Pitzer moments of inertia indicates that torsional coupling is important in the kinetic energy term as well as in the potential coupling. For R1 TS, the MS-RC(UC) and MS-RC(U) partition functions differ by a factor 2.5–2.6 for $T = 200$ –2400 K.

Figure 2 plots the ratio of the MS-T(C) partition function to the MS-T(U) partition function for various systems. It shows that the MS-T(C) partition functions are generally lower than those obtained by the MS-T(U) method. As the number of torsions involved in the anharmonic treatment increases, so do the differences between the two methods, especially at intermediate temperatures (500–2400 K). Although it is not

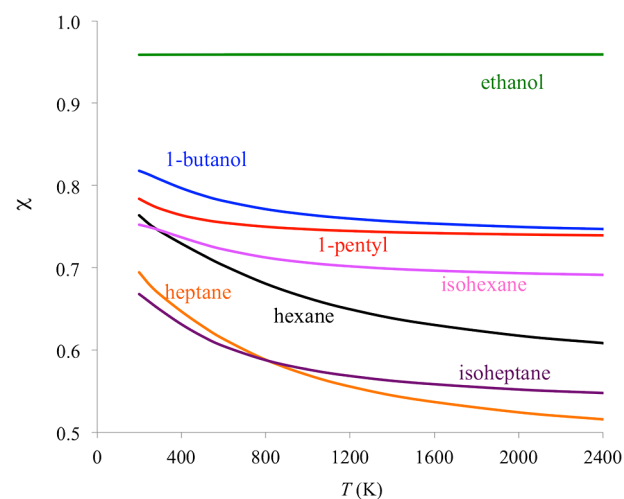
**Figure 2.** The ratio of the MS-T(C) partition function to the MS-T(U) partition function for various species.

shown in Figure 2, if one continues the plot to higher temperatures the curves slowly rise to unity, and we get the same result by the two methods in the high- T limit.

For interpretive purposes, we define the ratio of the classical harmonic coupled torsional partition function to the classical harmonic uncoupled torsional partition function as

$$\chi = \frac{\sum_{j=1}^J \exp(-\beta U_j) \prod_{\eta=1}^t \hbar \beta \omega_{j,\eta}^{(C)}}{\sum_{j=1}^J \exp(-\beta U_j) \prod_{\tau=1}^t \hbar \beta \bar{\omega}_{j,\tau}} \quad (39)$$

This ratio is plotted for various species in Figure 3 to explore the source of the difference between the MS-T(U) and MS-

**Figure 3.** Ratio of the classical harmonic coupled torsional partition function to classical harmonic uncoupled torsional partition function for various species. This ratio is calculated by eq 39.

T(C) methods. The curves in Figure 3 agree qualitatively with those in Figure 2. Therefore, the differences between MS-T(C) and MS-T(U) methods are mainly caused by the different (coupled or uncoupled) torsional frequencies used in the $f_{j,\eta}$ or $f_{j,\tau}$ factors, at least for the cases in this study. The other factors that cause the difference between the two methods are the Z_j factors in the MS-T(U) method and different effective torsional

barriers used. Note that the Z_i factors in the MS-T(U) method are usually between 0.9 and 1.0 for the cases studied in this article. Harmonic frequencies used in the classical harmonic oscillator factors are lowered by including coupling between torsions in the MS-T(C) method; the classical harmonic oscillator torsional partition functions are increased by this. Because the classical HO partition functions are used in denominator to cancel corresponding parts of the quantum HO partition function, this decreases the MS-T(C) partition functions.

Also note that at the high-temperature limit, the partition functions obtained by both methods agree with each other because the free rotor partition function is independent of the frequencies and depends only on the moments of inertia.

The standard-state entropy and constant-pressure heat capacity differences between the MS-T(C) and MS-T(U) methods for various systems are plotted in Figures 4 and 5, respectively. If one continued Figure 4 up to high temperatures, one would see the results tend to the high- T limit of 0.

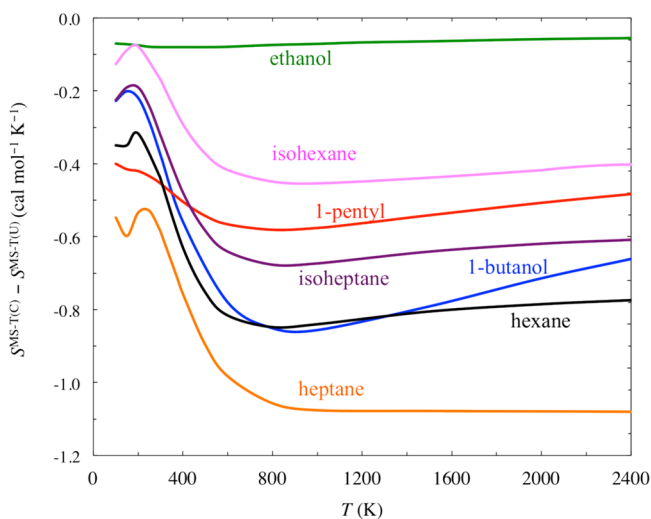


Figure 4. Standard state entropy difference between the MS-T(C) and MS-T(U) methods for various systems.

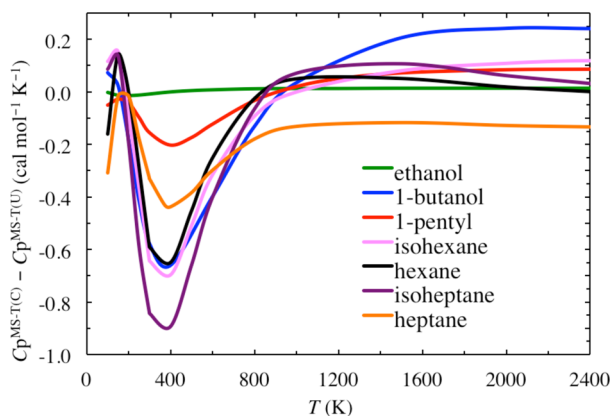


Figure 5. Standard-state, constant-pressure heat capacity difference between the MS-T(C) and MS-T(U) methods for various systems.

The standard-state entropy and constant-pressure heat capacity for certain temperatures and species are listed in Table 5 for comparison with experimental values. Entropies calculated by the MS-T(C) method are usually lower than

Table 5. Comparison of Calculated Thermodynamic Functions to Experimental Values

T (K)	MS-T(U)	MS-T(C)	exptl.
entropy S° (cal mol ⁻¹ K ⁻¹)			
1-butanol			
298	87.34	87.02	86.8 ^a
heptane			
371.5	112.48	111.75	111.8 ^b
heat capacity C_p° (cal mol ⁻¹ K ⁻¹)			
hexane			
333.85	38.26	37.60	37.35 ^c
365.15	41.02	40.34	40.22 ^c
398.85	43.94	43.29	43.30 ^c
433.70	46.88	46.29	46.39 ^c
468.90	49.72	49.20	49.46 ^c
isohexane			
325.10	37.70	37.00	36.77 ^d
362.15	41.21	40.49	40.30 ^d
402.25	44.89	44.20	44.08 ^d
436.20	47.85	47.22	47.14 ^d
471.15	50.75	50.18	50.16 ^d

^aFrom ref 54. ^bThe experimental data are from ref 55, and we added 0.026 cal mol⁻¹ K⁻¹ to convert from a standard pressure of 1 atm to a standard pressure of 1 bar. ^cFrom ref 56. ^dFrom ref 57.

those calculated by the MS-T(U) method. Compared with two experimental values for 1-butanol and heptane (see Table 5), the differences made by the MS-T(C) method are in the right direction.

Figure 5 shows that the largest heat capacity differences between these two methods occur around 300–400 K. Table 5 also lists experimental heat capacities for hexane and isohexane for this temperature range. We see that the MS-T(C) method improves both the hexane and isohexane cases and agrees with experimental values within 0.3 cal mol⁻¹ K⁻¹ for this temperature region. Also the temperature dependence of the heat capacity by the MS-T(C) method is improved for both cases compared with the experimental values.

5. CONCLUDING REMARKS

In this article, we present an improved formula for the multistructural method with torsional anharmonicity for calculating conformational-rovibrational partition functions and thermodynamic functions. The new formula is based on locally coupled torsional potentials whereas the original one was based on locally uncoupled torsional potentials, that is, on consideration of the potential only along separable internal coordinates and separable normal mode coordinates. The new formula eliminates the complicated Z_i switching functions of the original formula. We also assess the accuracy of the multistructure classical reference partition function [MS-RC(C)] against the fully coupled classical integral for two cases, pentane and the R1 saddle point. The assessment shows that the MS-RC(C) method significantly improves the accuracy if the coupled torsional effective barriers are used, and this suggests that the MS-T(C) scheme provides a better estimate of the partition function than the earlier MS-T(U) scheme when torsional–torsional coupling is especially important. The thermodynamic functions for four molecules tested (1-butanol, hexane, isohexane, and heptane) are all improved by the new MS-T(C) method.

AUTHOR INFORMATION

Corresponding Author

*E-mail: truhlar@umn.edu.

Notes

The authors declare no competing financial interest.

Nomenclature

C, coupled (effective barrier), coupled (moments of inertia), or consistently coupled (torsional frequency); CHO(C), classical harmonic oscillator using consistently coupled frequencies; CHO(U), classical harmonic oscillator using uncoupled frequencies; FCC, fully coupled classical-limit (method); HO, harmonic oscillator; KP, Kilpatrick and Pitzer (moments of inertia); MS, multistructural (method); MS-LH, multistructural local-harmonic (method); MS-LQ, multistructural local-quasi-harmonic (method); MS-RC(C), multistructural reference classical (method using) coupled (effective barriers and coupled moments of inertia); MS-RC(U), multistructural reference classical (method using) uncoupled (effective barriers and uncoupled moments of inertia); MS-RC(UC), multistructural reference classical (method using) uncoupled (effective barriers and) coupled (moments of inertia); MS-AS, multistructural all-structures (method); MS-T, multistructural (method for) torsions; MS-T(C), multistructural (method for) torsions—coupled (that is, using consistently coupled torsional frequencies, coupled effective barriers, and coupled moments of inertia); MS-T(U), multistructural (method for) torsions—uncoupled (that is, using uncoupled torsional frequencies, uncoupled effective barriers, and uncoupled moments of inertia, but with the coupling between torsional frequencies and moments of inertia considered in the Z_i factor); PC, primitively coupled (frequency); RC(C), reference classical (method for torsions)—coupled (that is, using coupled effective barriers and coupled moments of inertia); RC(U), reference classical (method for torsions)—uncoupled (that is, using uncoupled effective barriers and uncoupled moments of inertia); RC(UC), reference classical (method using) uncoupled (effective barriers) and coupled (moments of inertia); RPG, reference Pitzer—Gwinn (method); TS, transition state; U, uncoupled

ACKNOWLEDGMENTS

The authors are grateful to Steven Mielke for many helpful comments. This work was supported in part by the U.S. Department of Energy, Office of Science, Office of Basic Energy Science through the Combustion Energy Frontier Research Center under Award Number DE-SC0001198 and through grant no. DE-FG02-86ER13579.

REFERENCES

- (1) Pitzer, K. S. *Quantum Chemistry*; McGraw-Hill: Englewood Cliffs, NJ, 1953; pp 205–278.
- (2) Truhlar, D. G. *J. Comput. Chem.* **1991**, *12*, 266–270.
- (3) East, A. L. L.; Radom, L. *J. Chem. Phys.* **1997**, *106*, 6655–6674.
- (4) McClurg, R. B.; Flagan, R. C.; Goddard, W. A., III. *J. Chem. Phys.* **1997**, *106*, 6675–6680; **1999**, *111*, 7165–7165(E).
- (5) Ayala, P. Y.; Schlegel, H. B. *J. Chem. Phys.* **1998**, *108*, 2314–2325.
- (6) Masgrau, L.; González-Lafont, A.; Lluch, J. M. *J. Comput. Chem.* **2003**, *24*, 701–706.
- (7) Katzer, G.; Sax, A. F. *J. Comput. Chem.* **2005**, *26*, 1438–1451.
- (8) Wong, B. M.; Green, W. H., Jr. *Mol. Phys.* **2005**, *103*, 1027–1034.
- (9) Ellingson, B. A.; Lynch, V. A.; Mielke, S. L.; Truhlar, D. G. *J. Chem. Phys.* **2006**, *125*, 084305/1–17.
- (10) Vansteenkiste, P.; Verstraelen, T.; Van Speybroeck, V.; Waroquier, M. *Chem. Phys.* **2006**, *328*, 251–258.
- (11) Wong, B. M.; Thom, R. L.; Field, R. W. *J. Phys. Chem. A* **2006**, *110*, 7406–7413.
- (12) Pfaendtner, J.; Yu, X.; Broadbelt, L. J. *Theor. Chem. Acc.* **2007**, *118*, 881–898.
- (13) Lin, C. Y.; Izgorodina, E. I.; Coote, M. L. *J. Phys. Chem. A* **2008**, *112*, 1956–1964.
- (14) Bitencourt, A. C. P.; Ragni, M.; Maciel, G. S.; Aquilanti, V.; Prudente, F. V. *J. Chem. Phys.* **2008**, *129*, 154316/1–9.
- (15) Strekalov, M. L. *Chem. Phys.* **2009**, *362*, 75–81.
- (16) Nagy, B.; Szakács, P.; Csontos, J.; Rolik, Z.; Tasi, G.; Kállay, M. *J. Phys. Chem. A* **2011**, *115*, 7823–7833.
- (17) Bloino, J.; Biczysko, M.; Barone, V. *J. Chem. Theory Comput.* **2012**, *8*, 1015–1036.
- (18) Zheng, J.; Yu, T.; Papajak, E.; Alecu, I. M.; Mielke, S. L.; Truhlar, D. G. *Phys. Chem. Chem. Phys.* **2011**, *13*, 10885–10907.
- (19) Zheng, J.; Mielke, S. L.; Clarkson, K. L.; Truhlar, D. G. *Comput. Phys. Commun.* **2012**, *183*, 1803–1812.
- (20) Yu, T.; Zheng, J.; Truhlar, D. G. *Chem. Sci.* **2011**, *2*, 2199–2213.
- (21) Zheng, J.; Yu, T.; Truhlar, D. G. *Phys. Chem. Chem. Phys.* **2011**, *13*, 19318–19324.
- (22) Yu, T.; Zheng, J.; Truhlar, D. G. *Phys. Chem. Chem. Phys.* **2011**, *14*, 482–494.
- (23) Yu, T.; Zheng, J.; Truhlar, D. G. *J. Phys. Chem. A* **2012**, *116*, 297–308.
- (24) Seal, P.; Papajak, E.; Yu, T.; Truhlar, D. G. *J. Chem. Phys.* **2012**, *136*, 034306/1–10.
- (25) Xu, X.; Papajak, E.; Zheng, J.; Truhlar, D. G. *Phys. Chem. Chem. Phys.* **2012**, *14*, 4204–4216.
- (26) Alecu, I. M.; Truhlar, D. G. *J. Phys. Chem. A* **2011**, *115*, 14599–14611.
- (27) Seal, P.; Papajak, E.; Truhlar, D. G. *J. Phys. Chem. Lett.* **2012**, *3*, 264.
- (28) Zheng, J.; Truhlar, D. G. *Faraday Discuss.* **2012**, *157*, 59–88.
- (29) Zheng, J.; Rocha, R. J.; Pelegrini, M.; Ferrão, L. F. A.; Carvalho, E. F. V.; Roberto-Neto, O.; Machado, F. B. C.; Truhlar, D. G. *J. Chem. Phys.* **2012**, *136*, 184310/1–10.
- (30) Zheng, J.; Seal, P.; Truhlar, D. G. *Chem. Sci.* **2012**, *4*, 200–212.
- (31) Kilpatrick, J. E.; Pitzer, K. S. *J. Chem. Phys.* **1949**, *17*, 1064–1075.
- (32) Pitzer, K. S. *J. Chem. Phys.* **1946**, *14*, 239–243.
- (33) Nguyen, K. A.; Jackels, C. F.; Truhlar, D. G. *J. Chem. Phys.* **1996**, *104*, 6491–6496.
- (34) Eckart, C. *Phys. Rev.* **1935**, *47*, 552–558.
- (35) Sayvetz, A. *J. Chem. Phys.* **1939**, *6*, 383–389.
- (36) Wilson, E. B., Jr.; Decius, J. C.; Cross, P. C. *Molecular Vibrations*; McGraw-Hill: New York, 1955; pp 54–76.
- (37) Pitzer, K. S.; Gwinn, W. D. *J. Chem. Phys.* **1942**, *10*, 428–440.
- (38) Alecu, I. M.; Zheng, J.; Zhao, Y.; Truhlar, D. G. *J. Chem. Theory Comput.* **2010**, *6*, 2872–2887.
- (39) Pratt, L. M.; Truhlar, D. G.; Cramer, C. J.; Kass, S. R.; Thompson, J. D.; Xidos, J. D. *J. Org. Chem.* **2007**, *72*, 2962–2966.
- (40) Zhao, Y.; Truhlar, D. G. *Phys. Chem. Chem. Phys.* **2008**, *10*, 2813–2818.
- (41) Ribeiro, R. F.; Marenich, A. V.; Cramer, C. J.; Truhlar, D. G. *J. Phys. Chem. B* **2011**, *115*, 14556–14562.
- (42) Zheng, J.; Mielke, S. L.; Clarkson, K. L.; Truhlar, D. G. *MSTor*, modified based on version 2011–3-A; University of Minnesota: Minneapolis, MN, 2012.
- (43) Frisch, M. J.; Trucks, G. W.; Schlegel, H. B.; Scuseria, G. E.; Robb, M. A.; Cheeseman, J. R.; Scalmani, G.; Barone, V.; Mennucci, B.; Petersson, G. A.; Nakatsuji, H.; Caricato, M.; Li, X.; Hratchian, H. P.; Izmaylov, A. F.; Bloino, J.; Zheng, G.; Sonnenberg, J. L.; Hada, M.; Ehara, M.; Toyota, K.; Fukuda, R.; Hasegawa, J.; Ishida, M.; Nakajima, T.; Honda, Y.; Kitao, O.; Nakai, H.; Vreven, T.; Montgomery, J. A., Jr.; Peralta, J. E.; Ogliaro, F.; Bearpark, M.; Heyd, J. J.; Brothers, E.; Kudin, K. N.; Staroverov, V. N.; Kobayashi, R.; Normand, J.; Raghavachari, K.; Rendell, A.; Burant, J. C.; Iyengar, S. S.; Tomasi, J.; Cossi, M.; Rega, N.; Millam, J. M.; Klene, M.; Knox, J. E.; Cross, J. B.; Bakken, V.; Adamo, C.; Jaramillo, J.; Gomperts, R.; Stratmann, R. E.; Yazyev, O.;

Austin, A. J.; Cammi, R.; Pomelli, C.; Ochterski, J. W.; Martin, R. L.; Morokuma, K.; Zakrzewski, V. G.; Voth, G. A.; Salvador, P.; Dannenberg, J. J.; Dapprich, S.; Daniels, A. D.; Farkas, O.; Foresman, J. B.; Ortiz, J. V.; Cioslowski, J.; Fox, D. J. *Gaussian 09*, revision A.02; Gaussian, Inc.: Wallingford, CT, 2009.

(44) Adler, T. B.; Knizia, G.; Werner, H.-J. *J. Chem. Phys.* **2007**, *127*, 221106/1–4.

(45) Knizia, G.; Adler, T. B.; Werner, H.-J. *J. Chem. Phys.* **2009**, *130*, 054104/1–20.

(46) Manby, F. R. *J. Chem. Phys.* **2003**, *119*, 4607–4613.

(47) Zhao, Y.; Truhlar, D. G. *J. Chem. Theory Comput.* **2008**, *4*, 1849–1868.

(48) Zhao, Y.; Truhlar, D. G. *Theor. Chem. Acc.* **2008**, *120*, 215–241. Erratum: **2008**, *119*, 525.

(49) Lynch, B. J.; Fast, P. L.; Harris, M.; Truhlar, D. G. *J. Phys. Chem. A* **2000**, *104*, 4811–4815.

(50) Lynch, B. J.; Zhao, Y.; Truhlar, D. G. *J. Phys. Chem. A* **2003**, *107*, 1384–1388.

(51) Papajak, E.; Truhlar, D. G. *J. Chem. Theory Comput.* **2010**, *6*, 597–501.

(52) Papajak, E.; Truhlar, D. G. *J. Chem. Theory Comput.* **2011**, *7*, 10–18.

(53) Hehre, W. J.; Radom, L.; Schleyer, P. v. R.; Pople, J. A. *Ab Initio Molecular Orbital Theory*; Wiley: New York, 1986; pp 65–88.

(54) Counsell, J. F.; Hales, J. L.; Martin, J. F. *Trans. Faraday Soc.* **1965**, *61*, 1869–1875.

(55) Waddington, G.; Todd, S. S.; Huffman, H. M. *J. Am. Chem. Soc.* **1947**, *69*, 22–30.

(56) Waddington, G.; Douslin, D. R. *J. Am. Chem. Soc.* **1947**, *69*, 2275–2279.

(57) Waddington, G.; Smith, J. C.; Scott, D. W.; Huffman, H. M. *J. Am. Chem. Soc.* **1949**, *71*, 3902–3906.